DE GRUYTER OPEN

10.1515/bjdm-2015-0039

BALKAN JOURNAL OF DENTAL MEDICINE

BaSS

ISSN 2335-0245

Effective Cell Growth Potential of Mg-Based Bioceramic Scaffolds towards Targeted Dentin Regeneration

SUMMARY

New emerging approaches in tissue engineering include incorporation of metal ions involved in various metabolic processes, such as Cu, Zn, Si into bioceramic scaffolds for enhanced cell growth and differentiation of specific cell types. The aim of the present work was to investigate the attachment, morphology, growth and mineralized tissue formation potential of Dental Pulp Stem Cells (DPSCs) seeded into Mg-based glass-ceramic scaffolds with incorporated Zn and Cu ions. Bioceramic scaffolds containing Si 60%, Ca 30%, Mg 7.5% and either Zn or Cu 2.5%, sintered at different temperatures were synthesized by the foam replica technique and seeded with DPSCs for up to 21 days. Scanning Electron Microscopy with associated Energy Dispersive Spectroscopy (SEM-EDS) was used to evaluate their ability to support the DPSCs's attachment and proliferation, while the structure of the seeded scaffolds was investigated by X-Ray Diffraction Analysis (XRD). Zn-doped bioceramic scaffolds promoted the attachment and growth of human DPSCs, while identically fabricated scaffolds doped with Cu showed a cytotoxic behaviour, irrespective of the sintering temperature. A mineralized tissue with apatite-like structure was formed on both Cu-doped scaffolds and only on those Zn-doped scaffolds heat-treated at lower temperatures. Sol-gel derived Zn-doped scaffolds sintered at 890oC support DPSC growth and apatite-like tissue formation, which renders them as promising candidates towards dental tissue regeneration.

Keywords: Bioceramic Scaffolds; Dental Pulp Stem Cells; Copper Ions; Zinc Ions; Dentin Regeneration

E. Kontonasaki[1], A. Bakopoulou[1], A. Theocharidou[1], G. S. Theodorou[2], L. Papadopoulou[3], N. Kantiranis[2], M. Bousnaki[1], C. Chatzichristou[1], E. Papachristou[1], K.M. Paraskevopoulos[2], P. Koidis[1]

Aristotle University of Thessaloniki
[1]School of Dentistry, Department of Fixed Prosthesis and Implant Prosthodontics
[2]Faculty of Sciences, Department of Physics
[3]Faculty of Sciences, Department of Geology
Thessaloniki, Greece

ORIGINAL PAPER OP)
Balk J Dent Med, 2015; 19:75-85

Introduction

Scaffold-based approach for dental tissue regeneration involves the use of an appropriate scaffolding material where cells, triggered by specific molecular or environmental cues, become able to "create" tissues of the desired architecture. Ceramic scaffolds consisting of calcium/phosphate glasses, such as β-TCP and HA have been applied for tooth or specific dental tissue regeneration due to their compositional resemblance to hydroxyapatite, the mineral phase of enamel, dentin and cementum, while other bioactive glasses and glass ceramic compositions have shown promising results.

Magnesium (Mg) is a key element in human body, as it plays a significant role in cellular processes[1,2] and skeletal metabolism[3,4], while Mg deprivation inhibits cell growth[5]. Despite the effective use of Mg in bone tissue regeneration, Mg-containing glass-ceramics have been only recently proposed for dental tissue regeneration[6] and have been proven effective to induce differentiation of human mesenchymal stem cells (MSCs) [7]. The sustained release of Si and Mg during the gradual degradation of the scaffolds can significantly enhance proliferation, differentiation and bio-mineralization of stem cells as well as human dental pulp stem cells (DPSCs) in vitro[8].

Many trace elements, such as Sr, Cu, Zn or Co that are physiologically present in the human body are known for their contribution effects in bone metabolism[9,10], so new emerging approaches exploit the potential introduction of these ions into scaffolding materials for an enhanced therapeutic result. Among those, copper (Cu) has been proposed to modulate the proliferation and differentiation of human MSCs[11], while it is known to have a positive effect on angiogenesis[12]. However, the most dominant property of copper is its antibacterial activity against various Gram-positive and Gram-negative species[13,14]. Another element of interest is zinc (Zn), as Zn ions show anti-inflammatory effects and stimulate bone formation *in vitro* by activating protein synthesis in osteoblasts[15,16]. Zinc ions attain further antibacterial properties, that are related to the modulation of membrane-associated enzyme mechanisms[17] and antimicrobial activity that has been partially attributed to the hydrogen peroxide that is generated from the surface of ZnO crystals[18]. Furthermore, the release of Zn^{2+} from dental restorative glass-ionomer cements has been reported to provide local antimicrobial resistance and cariostatic protection[19].

The ability to support cell growth and differentiation is a prerequisite for a successful scaffold for guided tissue regeneration. However, the strategy of incorporating into the ceramic scaffolds ions with antimicrobial properties and/or proven contribution to specific growth-kinetic mechanisms could be highly beneficial and lead to more efficient tissue regeneration. Consequently, the aim of the present work was to investigate the attachment, morphology, growth and mineralized tissue formation potential of DPSCs seeded into Mg-based glass-ceramic scaffolds with incorporated Zn and Cu .

Materials and Methods

Scaffold Synthesis

Mg-based scaffolds of different compositions (Tab. 1) were synthesized by the foam-replica technique[20] using sol-gel derived glasses. The sol-gel solution was prepared by the following procedure: *Tetra-ortho*-silicate *(TEOS)* was added in the mixture of ultra pure H_2O and HNO_3 (2N) and stirred for approximately 30min until partial hydrolysis of TEOS occurred. Calcium nitrate tetrahydrate ($Ca(NO_3)_2{\cdot}4H_2O$), Magnesium nitrate hexahydrate ($Mg(NO_3)_2{\cdot}6H_2O$) and Zinc nitrate hexahydrate ($Zn(NO_3)_2{\cdot}6H_2O$) or Cupric nitrate hemipentahydrate ($Cu(NO_3)_2{\cdot}2{,}5H_2O$) were added to the mixture, allowing 50 min for the hydrolysis reaction complete at 60ºC. After the immersion of the foam in the sol-gel and mechanical stirring for 5 min, the samples (green bodies) were retrieved from the sol-gel and squeezed in order to remove the excess of sol from the pores and then left to dry out for at least 12 h. The thickness of the bioactive glass on the green bodies was adjusted by pouring droplets of sol-gel on them and making sure that the excess of it was removed after centrifuging the green bodies. Following, the synthesized scaffolds were sintered at different temperatures according to the Thermogravimetric (TG) and Differential Scanning Calorimetry (DSC) curves[21] (Tab. 1).

Table 1. Composition and sintering temperature of the synthesized scaffolds

Abbreviations	Compositions	Sintering Temperature
ZnA2	Si60% Ca30% Mg7.5% Zn2.5%	890ºC
ZnB2	Si60% Ca30% Mg7.5% Zn2.5%	1180ºC
CuA2	Si60% Ca30% Mg7.5% Cu2.5%	866ºC
CuB2	Si60% Ca30% Mg7.5% Cu2.5%	1060ºC

Evaluation of Cell Attachment and Morphology of DPSCs Seeded into the Scaffolds

DPSC cultures were established from third molars of young healthy donors aged 16-18 years old and extensively characterized for several stem cell markers, as previously published by our group[22]. The collection of the samples was performed according to the guidelines of the Institutional Review Board and the parents of all donors signed an informed consent form. For the establishment of cell cultures the enzymatic dissociation method was used[23]. Cells were expanded with a MEM (Minimum Essential Media) culture medium (Invitrogen), supplemented with 15% FBS (EU-tested, Invitrogen), 100 μm of L-ascormic acid phosphate and 1% antibiotics/antimycotics (=complete Culture medium-CCM) and incubated at 37ºC in 5% CO_2. Cultured DPSCs in passage numbers from 3-6 were used for all experiments.

To analyze cell attachment and morphology, DPSCs were spotted at low volume (100 μl) into the scaffolds at 10^6 cells/scaffold in 24 well-plates and allowed to attach for 45 min before being fully covered with 1200 μl CCM. Medium change was performed every 2-3 days during the entire experimental period. After 3, 7, and 14 days the scaffold/cell constructs were processed for Scanning Electron Microscopy-SEM (Jeol, Japan). Briefly, cell/scaffold complexes were washed twice with PBS and fixed with 3% glutaraldehyde (in 0.1M sodium cacodylate, pH 7.4 containing 0.1M sucrose). The specimens were subsequently dehydrated in a series of increasing concentrations of ethanol, completely dried by exposure to hexamethyldisilazane and carbon-coated for SEM observation.

In a second series of experiments, DPSCs were spotted at 10^6 cells/scaffold in 24 well-plates, as described previously, and exposed to CCM supplemented additionally with 1.8 mM monopotassiumphosphate (KH2PO4) and 5 mM b-glycerophosphate (b-GP), as external phosphate sources to allow mineralized tissue formation. Energy Dispersive X-ray analysis was simultaneously performed on scaffold/cell constructs for the investigation of any compositional alterations of the scaffolds during the cell culture process. X-ray diffraction analysis (XRD) was used in order to exam changes of scaffold's crystal structure and/or the structural properties of any mineralized tissue. For the XRD analysis a Philips (PW1710) diffractometer with Ni-filtered CuKa wave radiation was used.

Results

Scaffold Morphology

The scaffolds derived from the Cu compositions were very brittle and multiple fractured struts and pores were observed in the respective SEM micro-photographs (Fig. 1, *a* and *b*). On the contrary scaffolds with pore size of approximately 200-400 μm and interconnected pore structure were successfully fabricated *via* the foam replica technique for the Zn compositions (Fig. 1, *c* and *d*). Almost all pores remained open while blocked pores were rarely observed. The scaffolds presented a mean porosity around 80%[21]. Although scaffolds of both formulations contained traces of Mg and similar amounts of Si, higher amounts of Ca were found in the Cu-doped scaffolds as recorded by the EDS analysis.

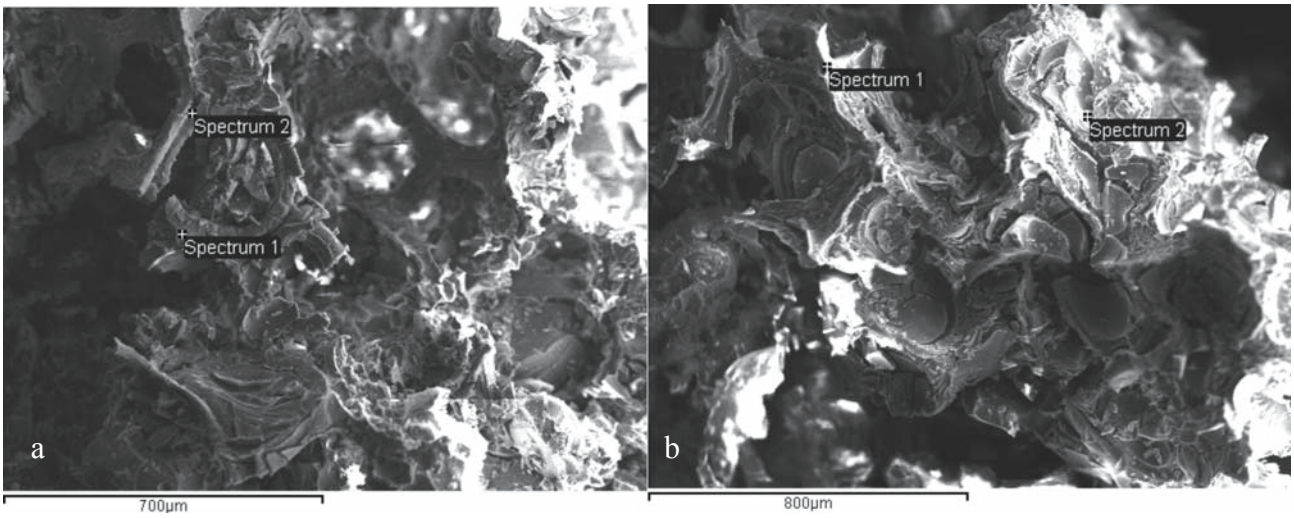

	CuA2 (a) w.t.%		CUB2 (b) w.t.%	
Element	Spectrum 1	Spectrum 2	Spectrum 1	Spectrum 2
O	41.40	32.71	44.37	53.63
Mg	1.17	1.15	1.54	2.66
Si	46.09	50.24	37.11	35.48
Ca	10.93	14.84	15.06	6.92
Cu	0.41	1.05	1.91	1.31
Totals	100.00	100.00	100.00	100.00

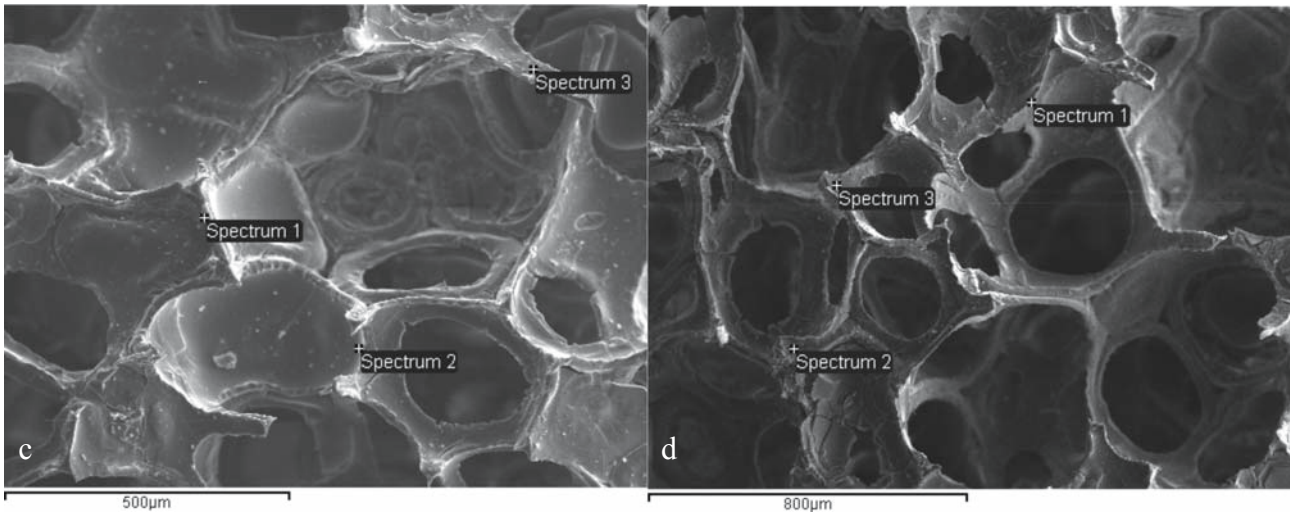

Element	ZnA2 (c) w.t.%			ZnB2 (d) w.t.%		
	Spectrum 1	Spectrum 2	Spectrum 3	Spectrum 1	Spectrum 2	Spectrum 3
O	25.77	33.92	43.08	51.67	46.82	48.95
Mg	0.99	0.75	0.75	1.01	0.69	0.40
Si	56.67	59.03	52.71	29.58	47.95	44.56
Ca	11.60	4.83	3.41	14.14	3.70	4.57
Zn	4.97	1.48	0.05	3.60	0.84	1.52
Totals	100.00	100.00	100.00	100.00	100.00	100.00

Figure 1. Representative SEM back-scattered micro-photographs of all types of scaffolds: (a) CuA2 (b) CuB2, (c) ZnA2 (d) ZnB2

Evaluation of Cell Attachment and Morphology of DPSCs Seeded into the Scaffolds

The SEM micro-photographs of representative scaffolds/cells constructs after 14 days of cell culture are presented in figure 2. It can be observed that cells attachment and growth were mainly favoured inside the struts and the pores of the ZnA2 scaffolds that were almost completely covered with cells after 14 days of culture. In contrast, only few cells were apparent on the surface of CuA2, CuB2 and ZnB2 scaffolds at all time points. Figure 2f reveals the significant attachment and spreading of DPSCs inside the ZnA2 scaffolds.

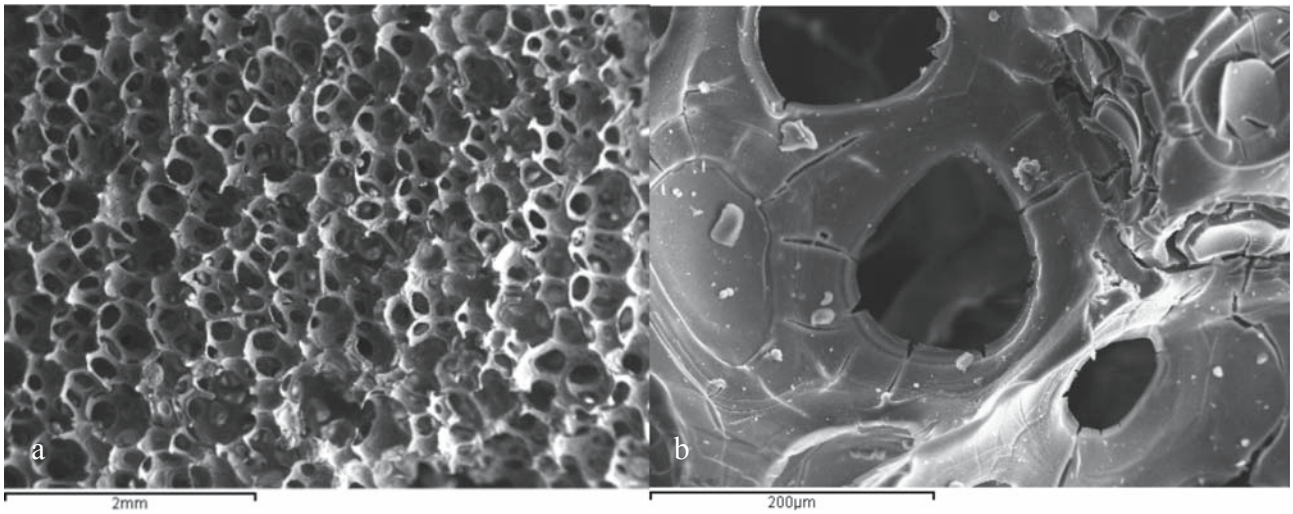

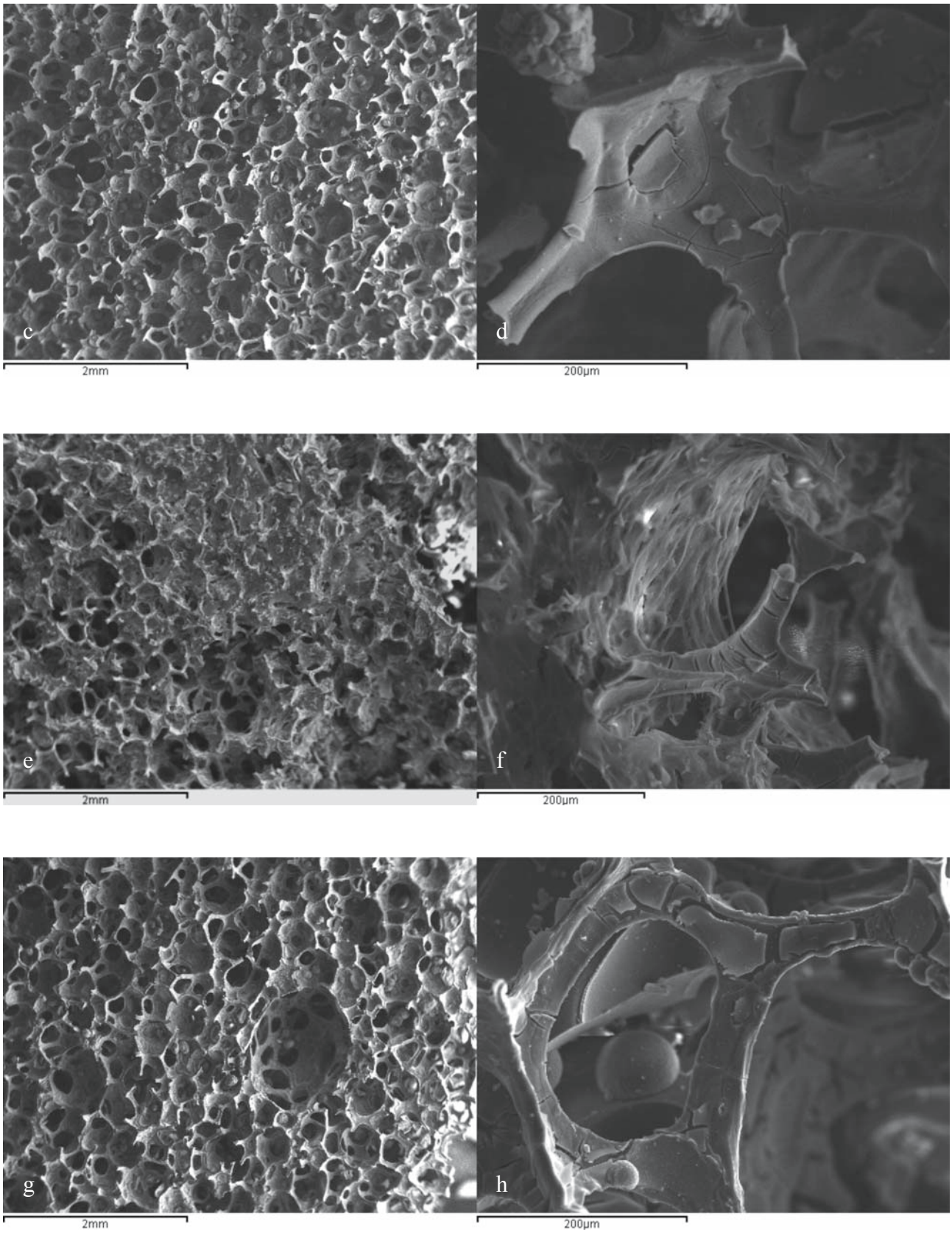

Figure 2. SEM micro-photographs of representative scaffolds/cells constructs after 14 days of culture. (a) CuA2, at lower and (b) CuA2 at higher magnification, (c) CuB2 at lower and (d) CuB2 at higher magnification, (e) ZnA2 at lower and (f) ZnA2 at higher magnification, (g) ZnB2 at lower and (h) ZnB2 at higher magnification

SEM micro-photographs with associated EDS analysis of the scaffolds/cells constructs after 21 days of culture in culture medium supplemented with external phosphate sources are presented in figures 3 and 4. The coloured frame in the back-scattered micro-photographs (Figures 3b, 3d, 4b, 4d) corresponds to the area of EDS analysis.

The whole surface of the scaffolds has been covered with a mineralized tissue that seals the pores, while no cells were apparent. In the case of Cu scaffolds, EDS analyses showed the presence of Ca, P and Si and no traces of Mg. Although Si and Ca could be found in the initial scaffold composition, the presence of P as well as a Ca/P ratio of the synthesized tissue ranging from 1.5-2.1, indicated formation of biological non-stoichiometric hydroxyapatite. This is further evidenced by the formation of multiple areas with mineralized aggregates on the surface of a CuA2 scaffold presented in the SEM micro-photograph in figure 5a. At higher magnification of a CuB2 scaffold, a fibrous-like tissue was observed with randomly developed mineralized nodules of apatite (Fig. 5b, spectrums 1,2).

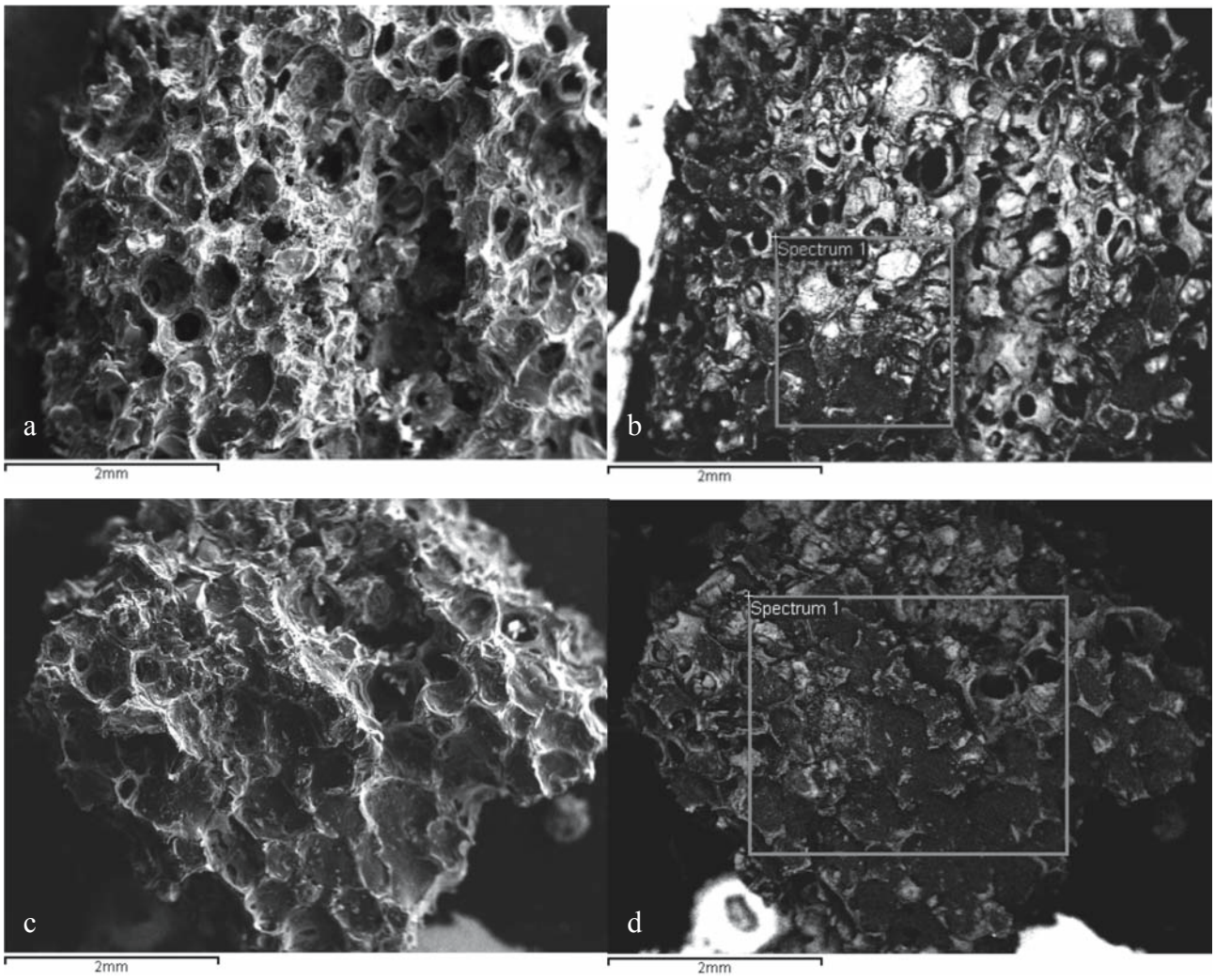

Element	CuA2 (b) %w.t.	CuB2 (d) %w.t.
O	42.50	46.04
Na	0.71	-
Si	39.14	40.59
P	5.71	5.34
Ca	11.95	8.04

Figure 3. Scaffolds/cell constructs after 21 days of culture: (a) SEM micro-photograph of a CuA2 scaffold seeded with DPSCs, (b) back-scattered micro-photograph of (a), (c) SEM micro-photograph of a CuB2 scaffold seeded with DPSCs, (d) back-scattered micro-photograph of (c). Frame corresponds to the area of EDS analysis

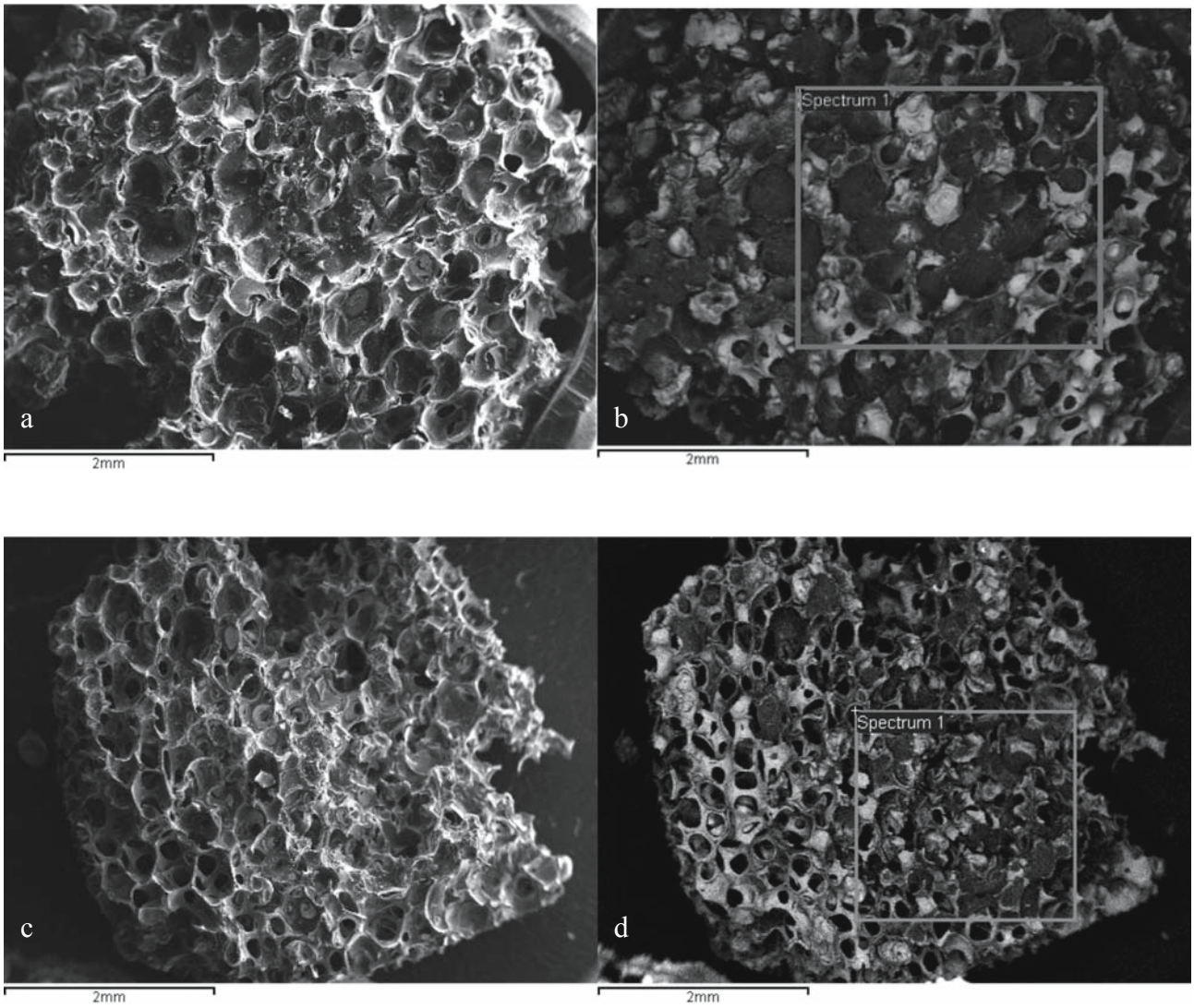

Element	ZnA2 (b) %w.t.	ZnB2 (d) %w.t.
O	42.9	44.23
Mg	-	0.14
Si	53.00	52.70
P	1.35	0.43
Ca	2.75	2.50
Total	100	100

Figure 4. Scaffolds/cell constructs after 21 days of culture: (a) SEM micro-photograph of a ZnA2 scaffold seeded with DPSCs, (b) back-scattered micro-photograph of (a), (c) SEM micro-photograph of a ZnB2 scaffold seeded with DPSCs, (d) back-scattered micro-photograph of (c). Frame corresponds to the area of EDS analysis.

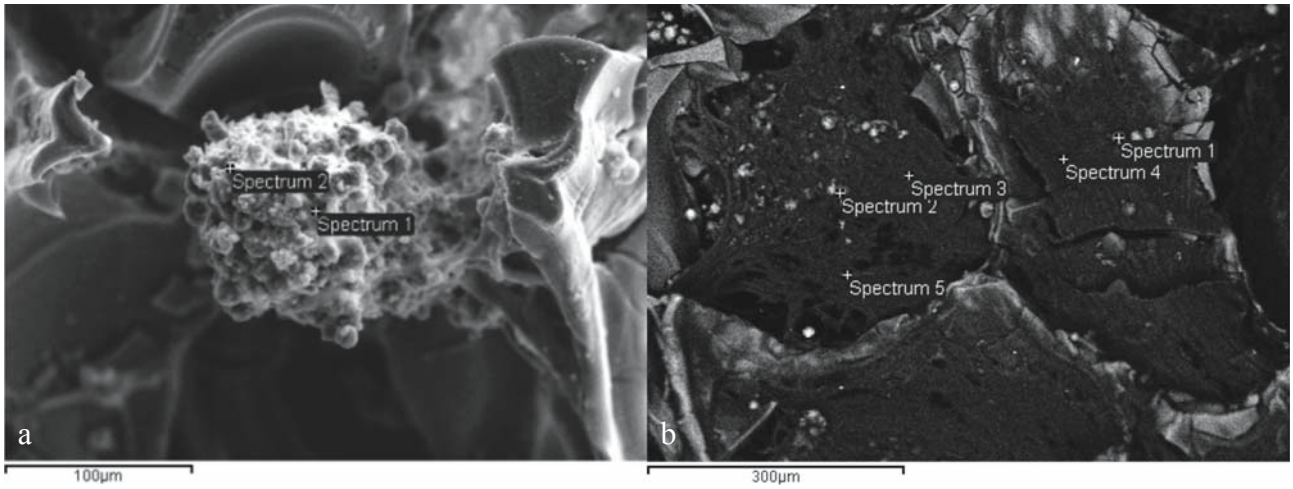

Element	CuA2 (a) (wt%)		CuB2 (b) (wt%)				
	Sp. 1	Sp. 2	Sp. 1	Sp. 2	Sp. 3	Sp. 4	Sp. 5
O	1.4	28.38	24.87	32.74	49.84	67.41	54.85
Na	-	-	0.86	1.72	-	-	-
Si	-	1.19	-		3.42	5.99	6.25
Mg	-	-	1.25	0.91	-	-	-
P	23.31	25.49	26.12	23.25	9.23	7.50	11.12
S	-	-	-	-	28.16	15.52	21.74
Ca	75.29	44.94	46.90	41.38	9.35	3.58	6.03
Total	100	100	100	100	100	100	100

Figure 5. (a) Backscattered microphototgraphs of a representative CuB2 scaffold, (b) Mineralized aggregates on a CuA2 scaffold.

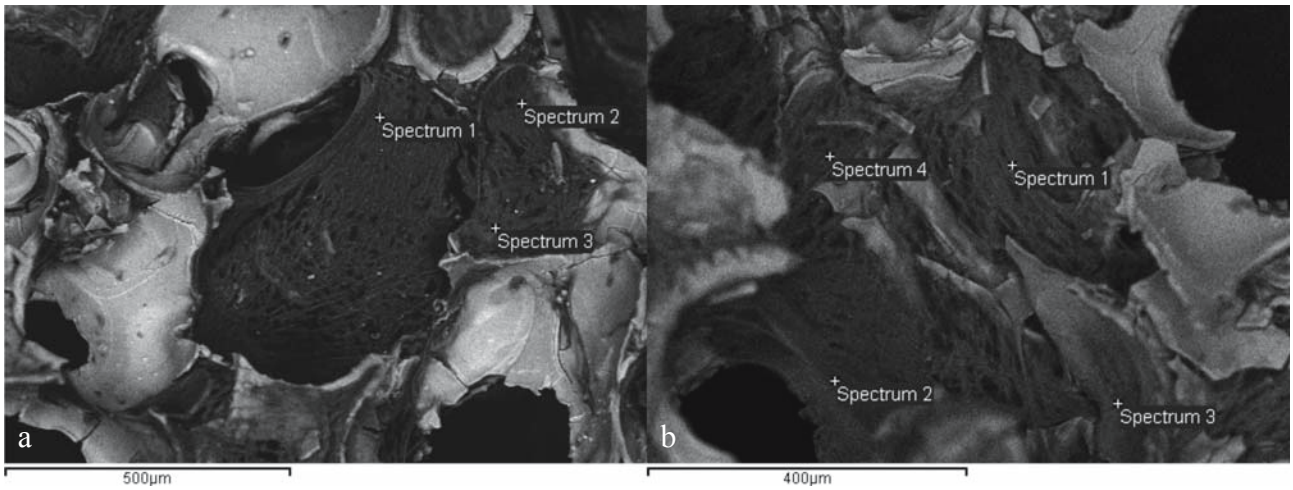

	ZnA2 (a) (w.t.%)			ZnB2 (b) (w.t.%)			
Elements	Sp.1	Sp.2	Sp.3	Sp.1	Sp.2	Sp.3	Sp.4
O	21.66	53.75	40.20	54.42	59.54	58.69	41.12
Na	4.88	6.30	3.85	6.26	3.73	4.71	5.37
Mg		1.47					0.02
Si	38.75	16.48	48.61	24.41	30.14	31.36	42.86
P	15.22	6.76	3.05	4.92	2.05	2.14	2.85
S		10.62	2.95	6.95	3.56	2.54	4.98
Ca	19.48	4.62	1.35	3.04	0.98	0.56	2.81
Totals	100	100	100	100	100	100	100

Figure 6. Backscattered microphototgraphs of a representative ZnA2 (a) and ZnB2 (b) scaffolds.

In contrast, only traces of Ca and P were found on the Zn scaffolds, although Ca and P were higher in ZnA2 compared to ZnB2 (Figure 4). Even though no apatitic phases were formed on Zn-doped scaffolds, backscattered micro-photographs revealed formation of a fibrous tissue similar to extracellular matrix that covered the whole surface of both ZnA2 and ZnB2 scaffolds and was well spread even inside their pores (Fig. 6, *a* and *b*).

The structure of the synthesized tissues was investigated through XRD and the results are presented in the respective XRD patterns in figure 7. For comparison reasons the XRD pattern of human dentine is apposed in the same figure. The formation of apatite is verified by a broad peak around 31° (2θ), showing the apatitic structure of the tissue formed on CuA2, CuB2 and to a lesser extent on ZnA2, while further, no other calcium phosphate phases were detected. Further, a higher amount of amorphous phase is present on the XRD patterns of both ZnA2 and ZnB2.

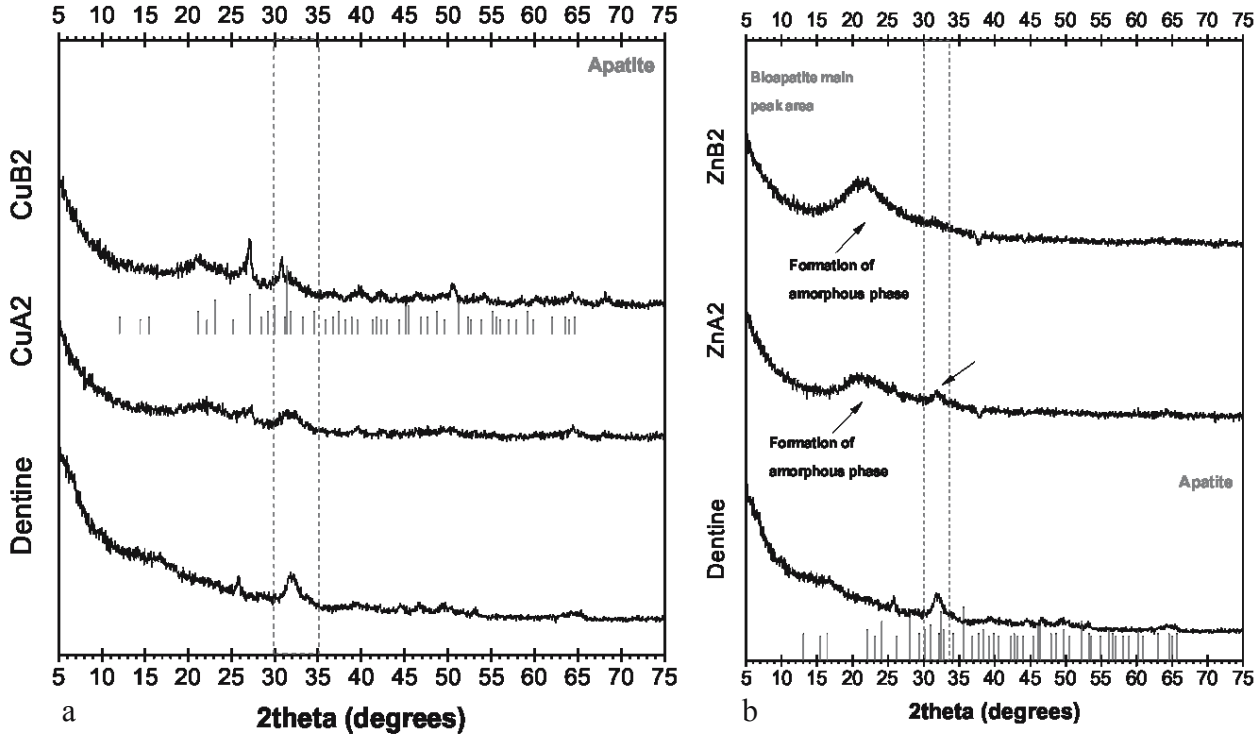

Figure 7. XRD patterns of the calcified tissues on the surface of the scaffolds remaining in culture for 21 days: (a) Cu-doped scaffolds, (b) Zn-doped scaffolds. The grey frame indicates the bioapatite main peak area

Discussion

This study investigated the efficacy of bioceramic scaffolds of different compositions to support the attachment, growth and mineralized tissue formation of human DPSCs up to 21 days in culture. SEM analysis revealed a much better biological behaviour of ZnA2 compared to all other scaffolds. The cells proliferated over the surface of the scaffold and were densely grown, attaining an elongated, spindle-like morphology, indicative of high viability. In contrast, cells inside the CuA2 and CuB2 scaffolds could not attach, spread and grow and the respective SEM micro-photographs revealed a cytotoxic effect.

The profound differences concerning the biological response of these scaffolds can be attributed to major differences concerning their structure and composition. The effect of zinc incorporation into the structure of various glasses with potential application in tissue engineering has been reported to affect the 2 main properties of such glasses, i.e. bioactivity and biocompatibility. Zinc has been found to drastically reduce the total dissolution rate of various formulations in different media[24,25] and this reduction is concentration-depend[24]. Goel et al[25]

reported on the effect of varying the Zn^{2+}/Mg^{2+} ratio on the structure and biodegradation of glasses in an alkali-free system designed in the glass forming region of diopside ($CaMgSi_2O_6$)-fluorapatite [$Ca_5(PO_4)_3F$]-TCP ($3CaO{\cdot}P_2O_5$). They found that the increasing Zn^{2+}/Mg^{2+} ratio decreases the chemical degradation of glasses as well as reduces their apatite forming ability. On the other hand, Aina et al[24] after investigating the effect of Zn content in different zinc-doped 45S5-derived systems concluded that only the glass containing 5 wt.% Zn presented at the same time reduced solubility, apatite forming ability and conditions allowing endothelial cell growth over a 6-day period. Unpublished data of our group concerning the apatite forming ability of these scaffolds reveal that both the formation of new more stable crystal phases, such as foshagite ($Ca4Si_3O_9(OH)_2$), calcite $CaCO_3$, wollastonite ($CaSiO_3$) and christobalite (SiO_2), together with the generation of a glass structure with higher network connectivity, are associated to a lower dissolution process[23] and the inhibition of the conversion from amorphous CaP to HA, as has been reported in other studies as well[26,27]. This low dissolution of Zn-doped scaffolds leading to low amounts of released Zn or other elements may have attributed to the superior biological response of these scaffolds, as high amounts of Zn have been reported to present cytotoxicity[28,29] .

On the other hand, Cu-doped 45S5 BG scaffolds exhibit high apatite forming ability, as proven by the rapid formation of a carbonated HA layer on their surface (3 days in SBF)[30] . Hoppe et al[30] reported that Cu^{2+} addition (up to 2.5 wt.% CuO) had no effect on the reactivity of the un-doped BG, as measured through immersion in SBF. The reason for this difference between Zn- and Cu-doped scaffolds is that Zn ions can act either as network formers or network modifiers depending on their coordination forming less or more stable structures respectively, while Cu ions that are network modifiers generate glass structures less chemically stable and dense than that generated by Zn^{+2} ions[29]. However, whether this inferior biological behaviour of CuA2 scaffolds is due to a very high release of cytotoxic concentrations of Cu or any other elements or other underlying molecular mechanisms are responsible needs further investigation.

The formation of a mineralized tissue was evidenced in most of the scaffolds synthesized in this study, although nodules and aggregates of apatite were found on the Cu-doped compositions. Despite this, the inferior cellular response of Cu-doped scaffolds reveals the necessity to modify their composition and/or structure in order to restrict the release of toxic elements without jeopardizing their apatite forming ability. In contrast, the enhanced cell viability on the Zn-doped scaffolds impels further research on their potential ability to induce odontogenic differentiation of DPSCs.

Conclusions

The present study showed that Mg-based bioceramic scaffolds doped with Zn enhance the attachment, growth and mineralized tissue formation by human DPSCs, while identically fabricated scaffolds doped with Cu are cytotoxic. A mineralized tissue attaining apatite-like structure was formed on both Cu-doped scaffolds and only on the Zn-doped scaffolds heat-treated at lower temperatures. Combining these findings it is concluded that sol-gel derived Zn-doped scaffolds with the composition of Si60%, Ca30%, Mg7.5%, Zn2.5% sintered at 890^{o}C acquire the desired properties and can be further evaluated towards dental tissue regeneration.

Acknowledgments. This study was conducted under the action Excellence II (Project: 5105) and funded by the European Union (EU) and National Resources.

References

1. *Rubin H*. The logic of the membrane, magnesium, mitosis (MMM) model for the regulation of animal cell proliferation. *Arch Biochem Biophys*, 2007; 458:16-23.
2. *Wolf FI, Fasanella S, Tedesco B, Torsello A, Sgambato A, Faraglia B, Palozza P, Boninsegna A, Cittadini A*. Regulation of magnesium content during proliferation of mammary epithelial cells (HC-11). *Front Biosci*, 2004; 9:2056-2062.
3. *Wallach S*. Effects of magnesium on skeletal metabolism. *Magnes Trace Elem,* 1990; 9:1-14.
4. *Rude RK, Olerich M*. Magnesium deficiency: possible role in osteoporosis associated with gluten-sensitive enteropathy. *Osteoporos Int*, 1996; 6:453-461.
5. *Rubin H*. Magnesium: the missing element in molecular views of cell proliferation control. *Bioassays*, 2005; 27:311-320.
6. *Goudouri OM, Theodosoglou E, Kontonasaki E, Will J, Chrissafis K, Koidis P, Paraskevopoulos KM, Boccaccini AR*. Development of highly porous scaffolds based on bioactive silicates for dental tissue engineering. *Mater Res Bulletin*, 2014; 49:399-404.
7. *Huang Y, Jin X, Zhang X, Sun H, Tu J, Tang T, Chang J, Dai K*. In vitro and in vivo evaluation of akermanite bioceramics for bone regeneration. *Biomaterials*, 2009; 30:5041-5048.
8. *Qu T, Jing J, Jiang Y, Taylor RJ, Feng JQ, Geiger B, Liu X*. Magnesium-containing nanostructured hybrid scaffolds for enhanced dentin regeneration. *Tissue Eng*, 2014; 20:2422-2433.
9. *Saltman PD, Strause LG*. The role of trace minerals in osteoporosis. *J Am Coll Nutr*, 1993; 12:384-389.
10. *Beattie JH, Avenell A*. Trace element nutrition and bone metabolism. *Nutr Res Rev*, 1992; 5(1):167-188.
11. *Rodríguez JP, Ríos S, González M*. Modulation of the proliferation and differentiation of human mesenchymal stem cells by copper. *J Cell Biochem*, 2002; 85(1):92-100.

12. *Wu C, Zhou Y, Xu M, Han P, Chen L, Chang J, Xiao Y*. Copper-containing mesoporous bioactive glass scaffolds with multifunctional properties of angiogenesis capacity, osteostimulation and antibacterial activity. *Biomaterials*, 2013; 34:422-433.
13. *Olczak T, Maszczak-Seneczko D, Smalley J, Olczak M*. Gallium(III), cobalt(III) and copper(II) protoporphyrin IX exhibit antimicrobial activity against Porphyromonas gingivalis by reducing planktonic and biofilm growth and invasion of host epithelial cells. *Arch Microbiol*, 2012; 194:719-724.
14. *Elguindi J, Wagner J, Rensing C*. Genes involved in copper resistance influence survival of Pseudomonas aeruginosa on copper surfaces. *J Appl Microbiol*, 2009; 106:1448-1455.
15. *Hyun-Ju S, Young-Eun C, Taewan K, Hong-In S, In-Sook K*. Zinc may increase bone formation through stimulating cell proliferation, alkaline phosphatase activity and collagen synthesis in osteoblastic MC3T3-E1 cells. *Nutr Res Pract*, 2010; 4:356-361.
16. *Neve A, Corrado A, Cantatore FP*. Osteoblast physiology in normal and pathological conditions. *Cell Tissue Res*, 2011; 343(2):289-302.
17. *Söderberg T, Sunzel B, Holm S, Elmros T, Hallmans G, Sjöberg S*. Antibacterial effect of zinc oxide in vitro. *J Plast Surg Hand Surg*, 1990; 24:193-197.
18. *Sawai J, Shoji S, Igarashi H, Hashimoto A, Kokugan T, Shimizu M, Kojima H*. Hydrogen peroxide as an antibacterial factor in zinc oxide powder slurry. *J Ferment Bioeng*, 1998; 86:521-522.
19. *Zoergiebel J, Ilie N*. Evaluation of a conventional glass ionomer cement with new zinc formulation: effect of coating, aging and storage agents. *Clin Oral Investig*, 2013; 17:619-626.
20. *Chen QZ, Thompson ID, Boccaccini AR*. 45S5 Bioglass (R)-derived glass-ceramic scaffolds for bone tissue engineering. *Biomaterials*, 2006; 27:2414-2425.
21. *Theodorou GS, Kontonasaki E, Theocharidou A, Bakopoulou A, Bousnaki M, Chatzichristou C, Papachristou E, Papadopoulou L, Kantiranis N, Chrissafis K, Paraskevopoulos KM, Koidis P*. Synthesis and study of biomimetic ceramic scaffolds towards dental stem cell differentiation and calcified dental tissue engineering. Submitted to *Mater Chem Phys*, February 2015.
22. *Paschalidis T, Bakopoulou A, Papa P, Leyhausen G, Geurtsen W, Koidis P*. Dental pulp stem cells' secretome enhances pulp repair processes and compensates TEGDMA-induced cytotoxicity. *Dent Mater*, 2014; 30:405-418.
23. *Bakopoulou A, Leyhausen G, Volk J, Tsiftsoglou A, Garefis P, Koidis P, Geurtsen W*. Assessment of the Impact of Two Different Isolation Methods on the Osteo/Odontogenic Differentiation Potential of Human Dental Stem Cells Derived from Deciduous Teeth. *Calcif Tissue Int*, 2011; 88(2):130-141.
24. *Aina V, Malavasi G, Fiorio PA, Munaron L, Morterra C*. Zinc-containing bioactive glasses: surface reactivity and behaviour towards endothelial cells. *Acta Biomater*, 2009; 5:1211-1222.
25. *Goel A, Kapoor S, Tilocca A, Rajagopal RR, Ferreira JMF*. Structural role of zinc in biodegradation of alkali-free bioactive glasses. *J Mater Chem B*, 2013; 1:3073-3082.
26. *Haimi S, Gorianc G, Moimas L, Lindroos B, Huhtala H, Räty S, Kuokkanen H, Sándor GK, Schmid C, Miettinen S, Suuronen R*. Characterization of zinc-releasing three-dimensional bioactive glass scaffolds and their effect on human adipose stem cell proliferation and osteogenic differentiation. *Acta Biomater*, 2009; 5:3122-3131.
27. *Bini M, Grandi S, Capsoni D, Mustarelli P, Saino E, Visai L*. SiO2-P2O5-CaO glasses and glass-ceramics with and without ZnO: relationships among composition, microstructure, and bioactivity. *J Phys Chem C*, 2009; 113: 8821-8828.
28. *Aina V, Perardi A, Bergandi L, Malavasi G, Menabue L, Morterra C, Ghigo D*. Cytotoxicity of zinc-containing bioactive glasses in contact with human osteoblasts. *Chem Biol Interact*, 2007; 167:207-218.
29. *Bejarano J, Caviedes P, Palza H*. Sol-gel synthesis and in vitro bioactivity of copper and zinc-doped silicate bioactive glasses and glass-ceramics. *Biomed Mater*, 2015; 10:025001.
30. *Hoppe A, Meszaros R, Stähli C, Romeis S, Schmidt J, Peukert W, Marelli B, Nazhat SN, Wondraczek L, Lao J, Jallotf E, Boccaccini AR*. In vitro reactivity of Cu doped 45S5 Bioglass® derived scaffolds for bone tissue engineering. *J Mater Chem B*, 2013; 1:5659-5674.

Correspondence and request for offprints to:

Prof. Petros Koidis
Aristotle University of Thessaloniki
University Campus, Dentistry Building
GR54124, Thessaloniki
Greece
E-mail: pkoidis@dent.auth.gr